European Journal of Pharmacology 939 (2023) 175453

Contents lists available at ScienceDirect

European Journal of Pharmacology

journal homepage: www.elsevier.com/locate/ejphar

The vasodilator naftidrofuryl attenuates short-term brain glucose hypometabolism in the lithium-pilocarpine rat model of status epilepticus without providing neuroprotection

Luis García-García [a,b,e,*], Francisca Gomez [a,b], Mercedes Delgado [c], Rubén Fernández de la Rosa [b,c], Miguel Ángel Pozo [b,d,e]

[a] Department of Pharmacology, Pharmacognosy and Botany. Faculty of Pharmacy, Complutense University of Madrid, Madrid, Spain
[b] Brain Mapping Unit, Instituto Pluridisciplinar, Complutense University of Madrid, Madrid, Spain
[c] BIOIMAC, Complutense University of Madrid, Madrid, Spain
[d] Department of Physiology, Faculty of Medicine, Complutense University of Madrid, Madrid, Spain
[e] Health Research Institute, Hospital Clínico San Carlos (IdISSC), Madrid, Spain

ARTICLE INFO

Keywords:
Lithium-pilocarpine model
[^{18}F]FDG PET
Glucose hypometabolism
Cerebral blood flow
Hippocampal damage
Neuroinflammation

ABSTRACT

Status epilepticus (SE) triggered by lithium-pilocarpine is a model of epileptogenesis widely used in rats, reproducing many of the pathological features of human temporal lobe epilepsy (TLE). After the SE, a silent period takes place that precedes the occurrence of recurrent spontaneous seizures. This latent stage is characterized by brain glucose hypometabolism and intense neuronal damage, especially at the hippocampus. Importantly, interictal hypometabolism in humans is a predictive marker of epileptogenesis, being correlated to the extent and severity of neuronal damage. Among the potential mechanisms underpinning glucose metabolism impairment and the subsequent brain damage, a reduction of cerebral blood flow has been proposed.

Accordingly, our goal was to evaluate the potential beneficial effects of naftidrofuryl (25 mg/kg i.p., twice after the insult), a vasodilator drug currently used for circulatory insufficiency-related pathologies. Thus, we measured the effects of naftidrofuryl on the short-term brain hypometabolism and hippocampal damage induced by SE in rats. 2-deoxy-2-[^{18}F]fluoro-D-glucose ([^{18}F]FDG) positron emission tomography (PET) neuroimaging along with various neurohistochemical assays aimed to assess brain damage were performed.

SE led to both severe glucose hypometabolism in key epilepsy-related areas and hippocampal neuronal damage. Although naftidrofuryl showed no anticonvulsant properties, it ameliorated the short-term brain hypometabolism induced by pilocarpine. Strikingly, the latter was neither accompanied by neuroprotective nor by anti-inflammatory effects. We suggest that naftidrofuryl, by acutely enhancing brain blood flow around the time of SE improves the brain metabolic state but this effect is not enough to protect from the damage induced by SE.

1. Introduction

Epilepsy is a chronic neurological disorder characterized by a persistent tendency to generate seizures and by its neurobiological, cognitive, psychological, and social consequences (Berg et al., 2010; Fisher et al., 2014). According to the World Health Organization, around 50 million people worldwide have epilepsy. Furthermore, it is estimated that up to 70% of epilepsy patients could live seizure-free if properly diagnosed and treated. Consequently, therapeutic tools to prevent or slow down the progression of the deleterious consequences of this disease are still needed.

Temporal lobe epilepsy (TLE) is the most predominant form of focal epilepsy in adults. It is frequently accompanied by hippocampal sclerosis (Janszky et al., 2005), being highly refractory to the current pharmacological treatments (Tang et al., 2017; Téllez-Zenteno and Hernández-Ronquillo, 2012). One hallmark of human TLE is the interictal glucose hypometabolism in the epileptogenic focus (Kumar and Chugani, 2017a, 2017b) that can be evaluated by 2-deoxy-2-[^{18}F]

* Corresponding author. Unidad de Cartografía Cerebral, Instituto Pluridisciplinar, Universidad Complutense de Madrid, Paseo Juan XXIII nº 1, 28040, Madrid, Spain.
E-mail address: lgarciag@ucm.es (L. García-García).

https://doi.org/10.1016/j.ejphar.2022.175453
Received 20 July 2022; Received in revised form 17 November 2022; Accepted 8 December 2022
Available online 11 December 2022

fluoro-D-glucose ([^{18}F]FDG) positron emission tomography (PET) imaging (Sarikaya, 2015).

One of the most used animal models of epilepsy is the lithium-pilocarpine rat model of status epilepticus (SE) (García-García et al., 2017, 2016; Kandratavicius et al., 2014; Leite et al., 2002; Shiha et al., 2015). This model reproduces hippocampal sclerosis as well as many other neuropathologic, electrographic and behavioral features of human TLE (Turski et al., 1983).

The SE induced by pilocarpine is followed by a seizure-free period characterized by a generalized brain glucose hypometabolism (García-García et al., 2017, 2016; Lee et al., 2012; Shiha et al., 2015). Besides, hypometabolism is concurrent with neurodegeneration, neuronal death, neuroinflammation and reactive gliosis (García-García et al., 2017; Rossi et al., 2013; Shapiro et al., 2008; Shiha et al., 2015). Brain hypometabolism has been attributed to neuronal death, diaschisis, reduction in synaptic density (Kumar and Chugani, 2017a, 2017b), and cerebral hypoperfusion (Bascuñana et al., 2021; Kumar and Chugani, 2017b). Regarding the latter, reduced brain hypoperfusion occurs shortly after pilocarpine administration, lasting at least for 12 weeks (Bascuñana et al., 2021).

Impaired cerebral blood flow might contribute to cognitive decline in epilepsy and in other neurological diseases (Daulatzai, 2017). Naftidrofuryl, (known as nafronyl in the US), is a vasodilator drug currently prescribed for the treatment of peripheral vascular disease, intermittent claudication, cerebral vascular disease and Raynoud's disease. Naftidrofuryl acts as an antagonist of the 5-hydroxytryptamine 2 (5-HT$_2$) receptors (Maloteaux et al., 1986; Wiernsperger, 1994), leading to vasodilation (Endemann et al., 2002; Oudart, 1990) and reduced platelet aggregation (Jagroop and Mikhailidis, 2000), therefore increasing brain perfusion (Young et al., 1983). Clinical studies indicate that naftidrofuryl seems to have beneficial effects on cognitive impairment conditions (Admani, 1978; Cox, 1975; Emeriau et al., 2000; Gerin, 1974; Judge and Urquhart, 1972; Lu et al., 2011).

To address whether naftidrofuryl might protect against some of the deleterious consequences of the SE in the rat lithium-pilocarpine model, we evaluated its effects on brain glucose metabolism during the early phase of epileptogenesis by [^{18}F]FDG PET. We also studied behavioral variables related to SE, as well as various histochemical markers associated with brain damage.

2. Materials and methods

2.1. Animals

A total of 40 adult male Sprague-Dawley rats (Charles River Laboratories Spain) weighing 293.1 ± 5.8 g at the beginning of the study were used. Rats were housed in standard rat cages (2 rats/cage), on a ventilated rack (Tecniplast, Italy) under controlled temperature (22 ± 2 °C) and a 12 h light/dark cycle (8:00 a.m.-8:00 p.m.). During the acclimation period as well as during the experimental procedure, rats had *ad libitum* access to standard rodent food, except for the 12h before the PET scans. The study was approved by the Animal Research Ethical Committee of the Universidad Complutense de Madrid, and it was carried out in accordance with regulations of the European Union (2010/63/UE) and Spain (RD53/2013) regarding animal welfare. All efforts were made to minimize, as much as possible, both the number of animals used and their suffering.

2.2. Lithium-pilocarpine model of SE

The procedure has been previously reported (García-García et al., 2017; Shiha et al., 2015). Briefly, lithium chloride (127 mg/kg i.p., Sigma–Aldrich) was administered 18–20 h before SE induction by pilocarpine. To minimize the peripheral effects of pilocarpine, methyl-scopolamine (2 mg/kg, i.p.) was administered 30 min previous to pilocarpine injection (25 mg/kg, i.p.; Sigma–Aldrich, St. Louis, MO). Regarding pilocarpine, the dose of 25 mg/kg has been used also by other research groups (Rigoulot et al., 2004; Walton and Treiman, 1988; Yang et al., 2014).

The convulsive behavior was evaluated according to the Racine scale (Racine, 1972). The onset of SE was considered when the animal reached the stage 4 (rearing with forelimb clonus) and showed continuous seizure activity. Rats stayed in seizure period for a maximum of 45 min and then it was ended by injecting pentobarbital (25 mg/kg, i.p.). The control rats that did not undergo SE were exposed to the same administration schedule, but saline solution (SAL) was used instead of drugs.

2.3. Naftidrofuryl administration

Naftidrofuryl (Sigma-Aldrich, St. Louis, MO) was i.p. administered at a dose of 25 mg/kg twice, dissolved in saline as vehicle. The first naftidrofuryl administration took place 5 min after the pilocarpine injection. The second dose was administered 8 h later. The dose of naftidrofuryl was selected based on previous studies reporting that similar doses had beneficial effects in brain stroke models (Miyake et al., 1993; Taguchi et al., 1994).

The final experimental groups were as follows: (1) control rats (SAL + VEH group, n = 7); (2) rats injected with pilocarpine (PILO + VEH group, n = 13); (3) rats injected with naftidrofuryl (SAL + NAFTI group, n = 7) and finally; (4) rats injected with both pilocarpine and naftidrofuryl (PILO + NAFTI group, n = 13). Three days after pilocarpine (or saline) injection, brain metabolism was evaluated by *in vivo* PET. One day later, the rats were sacrificed in order to carry out the different neurohistochemical evaluations. A diagram schematizing the timeline of the experimental procedures is depicted in Fig. 1.

2.4. [^{18}F]FDG PET neuroimaging

As stated before, to evaluate brain glucose metabolism, [^{18}F]FDG PET scans were carried out 3 days after the SE, during the silent period. Brain glucose hypometabolism can be detected as early as 3 days after SE (García-García et al., 2017; Shiha et al., 2015; Slowing et al., 2022) and it has been widely considered as an early marker of epileptogenesis (Shultz et al., 2013; Zhang et al., 2015). The protocols for image acquisition and processing have been previously detailed (García-García et al., 2018, 2017, 2016). A dual PET/CT (computed tomography) scanner was used (Albira scanner, Bruker NMI, Billerica, Massachusetts, U.S.A.). The radiotracer [^{18}F]FDG was injected into the tail vein (approximately 13 MBq–350 μCi-in 0.2 ml of 0.9%; Curium Pharma, Madrid, Spain). Thirty minutes later, rats were anesthetized by isoflurane, placed into the tomograph and the images acquired. The tomographic images were reconstructed and processed by PMOD 3.6 software (PMOD Technologies Ltd., Zurich, Switzerland). The steps for quantification of the metabolic activity were the following: (1) co-registration of the acquired images to a magnetic resonance image (MRI) rat brain template; (2) regional [^{18}F]FDG uptake images collection, (3) normalization of the uptake images to the standardized uptake value (SUV) based on the animal BW, the dose injected and the corrected [^{18}F]FDG uptake decay. The MRI rat brain template used for image co-registration and the volumes of interest (VOIs) corresponding to the brain areas for quantitation of metabolic activity are shown in Fig. 2.

2.5. Neurohistochemical assessments

Rats were sacrificed by decapitation the day after the PET acquisitions. Brains were dissected, cut longitudinally into two halves, frozen on dry ice, and stored at −80 °C. Brain slices (30 μm-thickness) from the left hemibrain were collected using a cryostat (Leica CM1850, Leica Biosystems, Germany). Sections containing the hippocampus (6 slices/slide) were thaw-mounted onto Superfrost Plus slides (Thermo Scientific, Germany), dried on a hot plate and stored into slide boxes at −80 °C

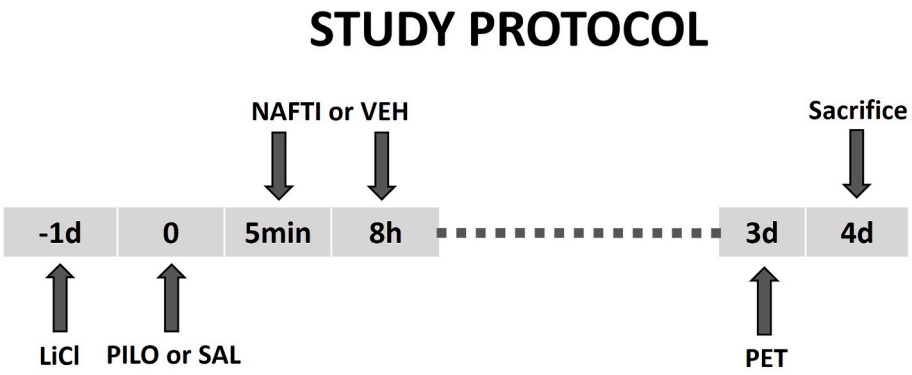

Fig. 1. Scheme of the experimental procedure of the study: LiCl (127 mg/kg) was administered 18–20 h before the induction of the SE. To induce the SE, 25 mg/kg pilocarpine (or saline in the control groups) was injected. Five min and 8 h after pilocarpine injection, naftidrofuryl (25 mg/kg, i.p.) or vehicle were administered. Three days later, to evaluate the regional brain glucose metabolism, PET/CT scans were carried out. The next day (day 4), the rats were sacrificed, and the brains removed to carry out the histochemical analyses.

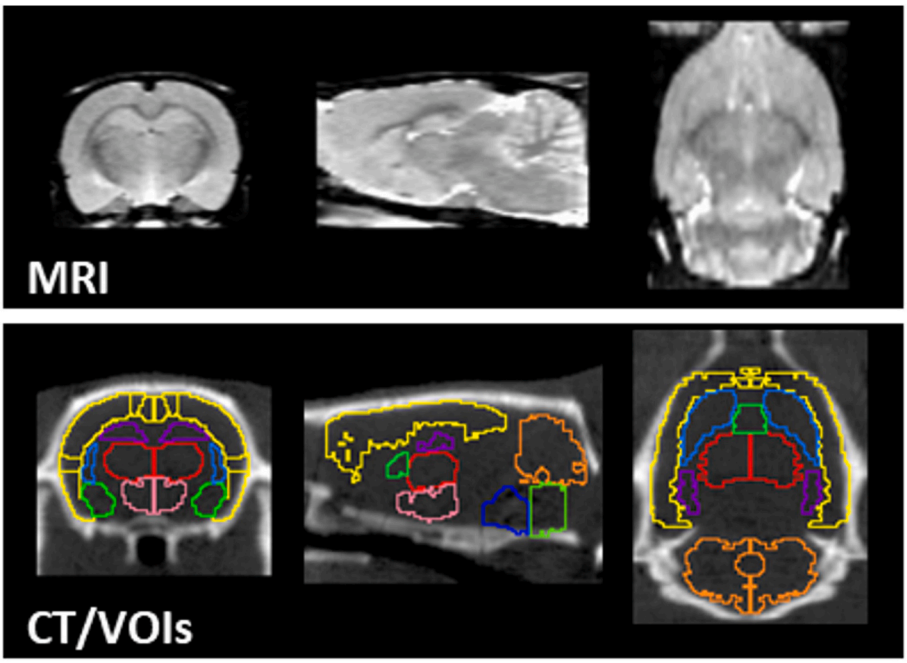

Fig. 2. The upper row shows the coronal, sagittal and transaxial views corresponding to the MRI brain template used for PET and CT images co-registration. The bottom row shows a sample CT image with the volumes of interest (VOIs) of the brain areas used for quantification of the regional metabolic activity by [18F] FDG PET.

until the day of the assays.

2.5.1. Neuronal viability and disruption of hippocampal integrity

Neuronal viability was evaluated by Nissl staining as previously described (García-García et al., 2018, 2017). Briefly, the slices were fixed in 4% formaldehyde in phosphate buffer pH 7.4 (10 min), washed in phosphate buffer (2 × 1 min) and incubated in 0.5% cresyl violet acetate solution (30 min). Afterwards, the sections were washed, dehydrated in graded ethanol series (70%, 95% and 100%) and cleared in xylene. Slices were cover-slipped with DPX mounting medium (Fluka, Switzerland). The images were captured with a digital camera (Leica DFC425, Leica, Germany) coupled to a microscope (Leica DM 2000 LED, Leica, Germany).

2.5.2. Hippocampal neurodegeneration

Neurodegeneration was evaluated by Fluoro-Jade C staining, as previously reported (García-García et al., 2017), following the original protocol with minor modifications ((Schmued et al., 2005). Briefly, The samples were fixed in 4% formaldehyde (10 min), rinsed in basic alcohol, 100% ethanol, distilled water, 0.06% potassium permanganate, 0.1% acetic acid solution containing 0.0001% Fluoro-Jade C (Millipore, Darmstadt, Germany), distilled water, and xylene. Then, the slides were cover-slipped with DPX (Fluka). The images were captured with a digital camera (Leica DFC3000G) coupled to a microscope (Leica DM 2000 LED) by using the FITC filter. At the hippocampal CA1, CA3 and hilus, the fluorescence signal was measured using ImageJ 1.46r software. The average value for each rat was calculated and the results were expressed as percentage *vs* the control group (VEH + SAL).

2.5.3. Reactive astrogliosis

Astrogliosis was evaluated by glial fibrillary acidic protein (GFAP) one-step immunofluorescence as previously reported (García-García et al., 2018, 2017). Briefly, the slices were formaldehyde-fixed, washed, blocked and permeabilized with 3% BSA, 0.1% triton X-100 in TBS (60 min) and incubated overnight with the anti-GFAP-Cy3 antibody (1:500, Sigma Aldrich) in 1% BSA in TBS at 4 °C. Afterwards, the slides were washed in 0.1% Tween 20 dissolved in Tween (3x for 5 min each) and cover-slipped with Mowiol. The images were captured and examined using the same optical systems used for Fluoro-Jade C, but in this case using the TRITC filter. For each brain section containing the CA1, CA3 and hilus areas at the anterior (dorsal) hippocampus the fluorescence intensity was measured (ImageJ 1.46r software). As with the

Fluoro-Jade C measurement, the average value for each rat was calculated and the results were expressed as percentage *vs* the control group (VEH + SAL).

2.5.4. Microglia-mediated neuroinflammation

Neuroinflammation mediated by activated microglia was studied by [^{3}H]PK11195 autoradiography as published (Foucault-Fruchard et al., 2017) with minor modifications. The slides were dried on a hot plate at 37 °C (10 min), preincubated with 50 mM Tris-HCl pH 7.4 at RT (15 min) and then incubated with 1 nM [^{3}H]PK11195 (Perkin Elmer) in preincubation buffer (60 min). Afterwards, the samples were washed in an ice cold preincubation buffer (2 × 5 min) and dipped in ice-cold distilled water. Once air-dried, the slides were exposed to Kodak Bio-Max MR autoradiography film (Carestream, U.S.A.) in an exposure cassette for approximately 2 months. After manual development, the film was placed onto a light box (Kaiser Prolite 5000, Kaiser Fototechnik, Germany) and the images captured with a camera (Leica DFC425) coupled to a stereomicroscope (Leica MZ6). The optical densities of the selected brain regions were used as index of neuroinflammation degree.

2.6. Statistical analyses

Analyses were performed with SigmaPlot 11.0 software (Systat Software Inc., Chicago, IL, U.S.A.). Behavioral markers of SE onset (latency) and mortality rate were only analyzed in the lithium-pilocarpine-treated rats (PILO + VEH *vs* PILO + NAFTI) by unpaired Student t-test and z-test for rates and proportions, respectively. Data from BW, PET neuroimaging and histochemical determinations were analyzed by two-way analysis of variance (ANOVA) followed by the post hoc Tukey test. In all cases, statistical significance was considered when $p < 0.05$. Data are shown as mean ± standard error of the mean (SEM).

3. Results

3.1. Behavioral and physiological changes

Naftidrofuryl administration neither modified the latency to SE, nor the number of seizures (Fig. 3A–B) in response to pilocarpine. In the current study, the mortality rate associated with SE was surprisingly low. In fact, there were no deaths in the PILO + VEH group, and only 2 of 13 rats from the PILO + NAFTI group died (death rate: 15.4%). The z-test for rates and proportions showed no significant differences between both groups ($p = 0.466$).

SE resulted in BW loss in the following 24h ($p<0.01$), the effect being independent of naftidrofuryl treatment (approximately 12% in PILO + VEH and 14% in PILO + NAFTI rats). The BW loss remained until the end of the experiment (Fig. 3C). When comparing the BW of both groups to their respective control groups (SAL + VEH and SAL + NAFTI) at the different time points, significant differences were also found (Fig. 3C).

3.2. Brain glucose metabolism

As depicted in Fig. 4A, glucose hypometabolism (measured as SUV) was detected, 3 days after the SE, in epilepsy-related brain areas. Compared to SAL + VEH, the SUV values in PILO + VEH were significantly reduced. Values ranged from 33.3% in midbrain ($p<0.001$) to 46.1% in striatum ($p<0.01$) (Fig. 4B). Specifically in our main area of interest, the hippocampus, the values went down 42.1% ($p<0.001$; Fig. 4B). Naftidrofuryl, in the absence of SE (SAL + NAFTI) had no significant effect on glucose brain metabolism. However, naftidrofuryl administration (PILO + NAFTI) significantly ameliorated the SE-

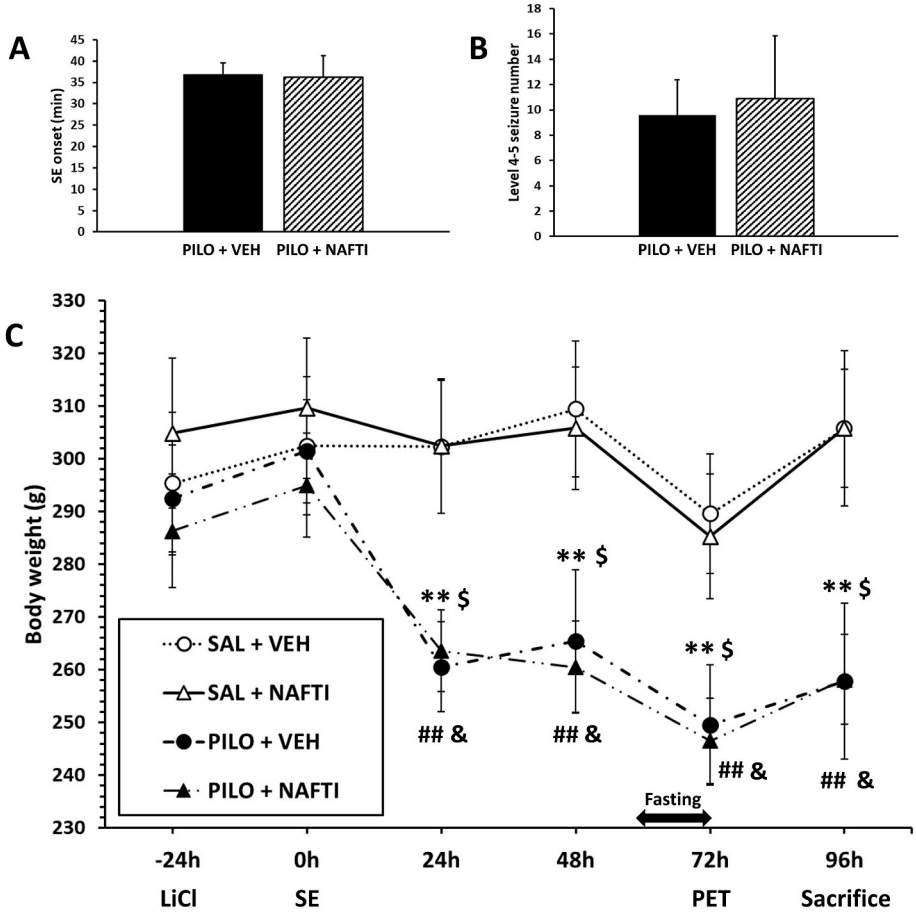

Fig. 3. (A) and (B) Naftidrofuryl did not show anticonvulsant effects on the SE triggered by pilocarpine administration, not affecting the latency time to SE (A) nor the number of seizures (B). (C) SE triggered by pilocarpine. (PILO + VEH group) resulted in a significant BW loss that was not prevented by previous administration of naftidrofuryl. Figures show the values as means ± SEM. **p<0.01, ##p<0.01 compared to their respective BW before pilocarpine injection (day 0); $p<0.05, &p<0.05 compared to their respective control groups (SAL + VEH and SAL + NAFTI, respectively); two-way ANOVAs followed by post-hoc Tukey test.

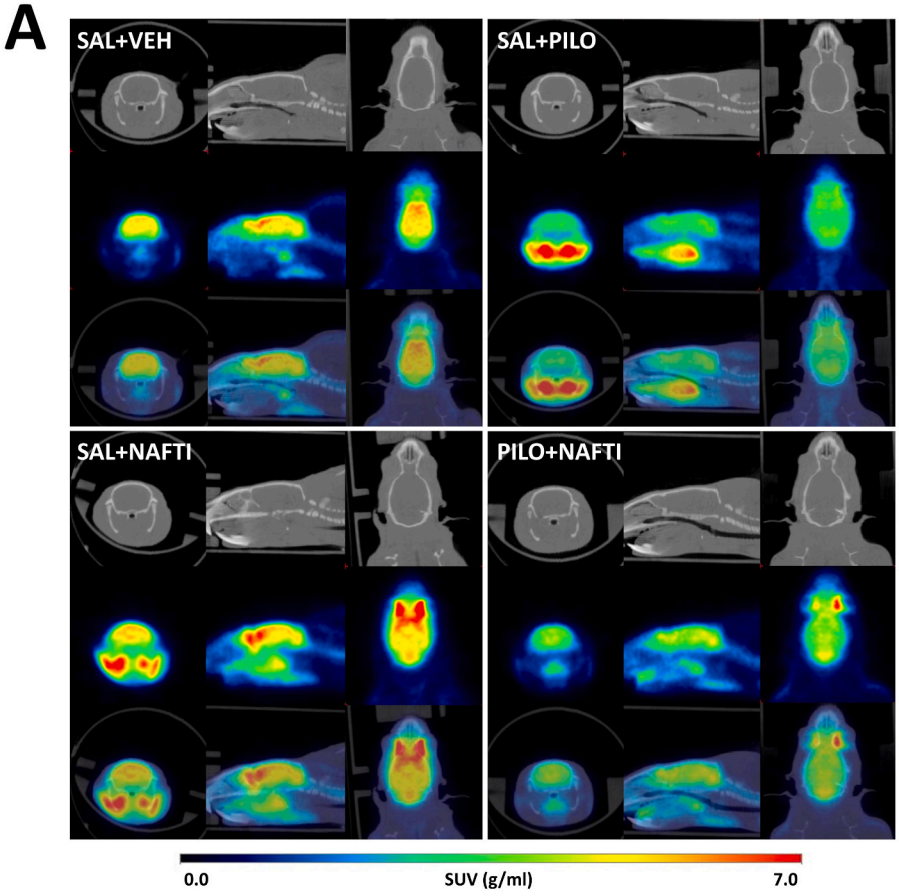

Fig. 4. SE induced by pilocarpine (PILO + VEH) induced a marked reduction of glucose metabolism in key areas involved in epileptogenesis, an effect that was partially ameliorated by naftidrofuryl. Regional brain glucose metabolism was evaluated by [^{18}F]FDG PET 3 days after the SE. **(A)** Representative CT (upper row), [^{18}F]FDG PET normalized to SUV scale (middle row) and merged PET/CT (bottom row) images in coronal, sagittal and trans-axial views of the 4 experimental groups. **(B)** Regional brain uptake in the 4 experimental groups is shown as SUV units (mean ± SEM); *p<0.05, **p<0.01 PILO + VEH *vs.* SAL + VEH and PILO + NAFTI *vs.* SAL + NAFTI; #p<0.05 PILO + NAFTI *vs.* PILO + VEH; two-way ANOVAs followed by post-hoc Tukey test.

induced hypometabolism in all brain regions studied, showing statistically significant higher SUV data (p<0.05; Fig. 4B).

3.3. Neurohistochemistry

As expected, neither signs of neurodegeneration, glial reactivity nor neuroinflammation were observable in SAL + VEH. Besides, naftidrofuryl administration in the absence of SE (SAL + NAFTI) had no effects in any of the variables studied.

Compared with its respective control group, SE triggered by pilocarpine (PILO + VEH) resulted in a visual loss of hippocampal neurons at the CA1, being this neuronal death lesser at the level of CA3, as shown by the cresyl violet micrographs (Fig. 5). As expected, there were also signs of hippocampal neurodegeneration, as revealed by a robust increase in Fluoro-Jade C labeling, measured as FITC fluorescence signal (Fig. 6A). The increase of fluorescence in CA1, CA3 and hilus areas was 10.8, 4.8 and 5.9 times compared with those found in the control group (p<0.05; Fig. 6B). Astrocytic activation in the different hippocampal areas, measured by GFAP immunofluorescence signal was also statistically significant; (p<0.001 in the three hippocampal areas analyzed; Fig. 7A). This increase in GFAP-TRITC signal ranged from 46% to 73% depending on the area. GFAP immunofluorescence in CA1 is shown in Fig. 7C. Regarding microglia-mediated neuroinflammation, SE in PILO + VEH rats resulted in an increase in the optical density obtained from the [^{3}H]PK11195 brain binding that ranged from 35% in thalamus to 61% in entorhinal cortex (Fig. 8A–B). In all the regions such increases were statistically significant (p<0.01 in hippocampus, entorhinal cortex and amygdala and p<0.05 in thalamus, parietal, and temporal cortices; Fig. 8B). It is noteworthy that brains of the pilocarpine-insulted rats show a marked edema formation at the level the piriform cortex, a typical feature of inflammation triggered by pilocarpine (Kim et al., 2010), especially at the level of the entorhinal and piriform cortices

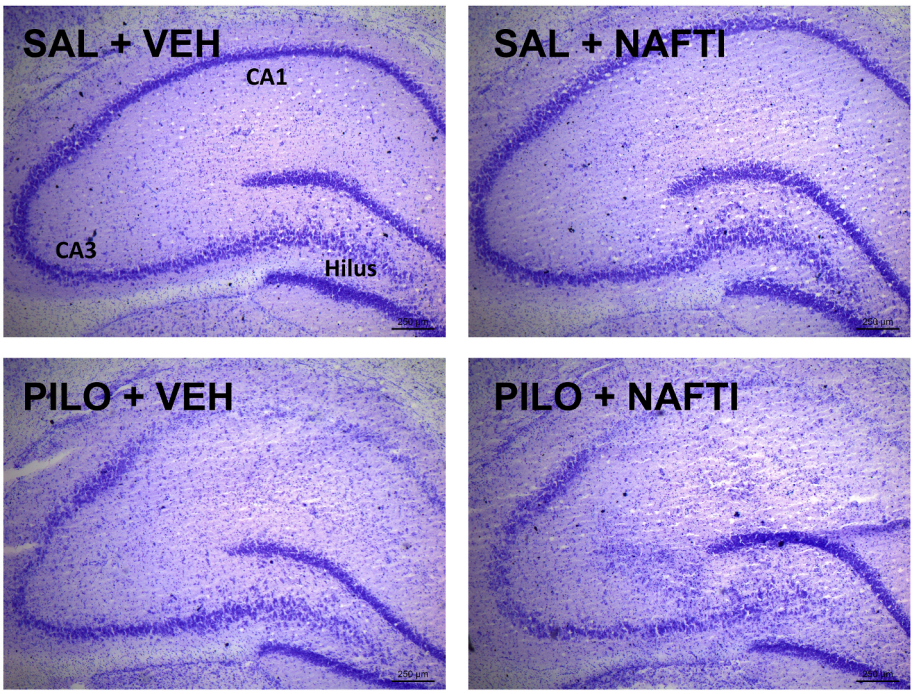

Fig. 5. Disruption of the hippocampal integrity produced by SE as visualized by cresyl violet (Nissl) staining. The micrographs show a severe damage induced by pilocarpine-triggered SE on the anterior hippocampus 72 h after pilocarpine injection both in the vehicle (PILO + VEH) and naftidrofuryl (PILO + NAFTI) treated groups.

(depicted by white arrows in Fig. 8B).

Noteworthy is the fact that naftidrofuryl administration failed to statistically modify any of the signs of hippocampal integrity disruption, neurodegeneration, glial reactivity or neuroinflammation induced by the SE (see Figs. 5–8).

4. Discussion

Herein, we have explored the effects of acute i.p. administration of naftidrofuryl on brain glucose metabolic dysfunction, hippocampal neurodegeneration and neuroinflammation, typical features of the brain damage associated to the SE in the rat lithium-pilocarpine model (García-García et al., 2017; Shiha et al., 2015). We have also studied its potential effects on latency to SE, mortality, and BW change.

Naftidrofuryl is a 5-HT_2 blocker that leads to vasodilation as well as reduction of platelet aggregation. At brain level, both actions result in enhanced blood flow (Young et al., 1983). Besides, in conditions of hypoxia, naftidrofuryl increases oxygen and energetic mediators' availability. Further, naftidrofuryl has been shown to improve aerobic glycolysis and to protect cell ATP reserves (Ogawa et al., 1991). Therefore, by reducing brain hypoperfusion-induced hypoxia, naftidrofuryl preserves metabolism and prevents neuronal death. Therefore, it is plausible that administration of naftidrofuryl might protect against some of the deleterious consequences of the SE.

In our study, acute naftidrofuryl treatment neither delayed the latency time, to the SE, number of seizures (Fig. 1A–B) nor affected the mortality rate consequence of the severity of SE induced by pilocarpine. In fact, the mortality rate associated to SE in this current study was very low. Based on our experience, using the same exact protocol, the death rate is commonly around 25–30%. However, other times it has been very high (Slowing et al., 2022). In any case it has been shown that the mortality rate associated to the severity of this model is hardly predictable, depending not only on the dose of pilocarpine, but also on factors such as rat strain, sub-strain, age, gender, commercial providers, and the time of purchase of animals (Buckmaster, 2004; Curia et al., 2008). In humans, seizures after parenteral administration of high doses of naftidrofuryl have been reported (Pohlmann-Eden et al., 1991). In animal models of epilepsy, anticonvulsant dose-dependent effects of naftidrofuryl have been reported in pentylenetetrazole (PTZ) kindled rats, but not in amygdala-kindled rats (Schmidt, 1990). In our study using the lithium-pilocarpine rat model of SE and after i.p. administration of 25 mg/kg twice, 5 min and 8 h after pilocarpine injection, naftidrofuryl had neither convulsant nor anticonvulsant effects. In this context it is important to bear in mind, that compared with the lithium-pilocarpine model of SE, the kindling models of epileptogenesis: (i) rely on repetitive chemical or electrical stimulation of limbic brain structures instead of on a single chemical insult; (ii) they lead to the onset seizures in a progressive manner instead of a rapid emergence of spontaneous seizures, and (iii) the neuropathological features are less severe and appear in a progressive cumulative therefore, more subtle effects might be detected (Becker, 2018; Samokhina and Samokhin, 2018). Accordingly, the effects of naftidrofuryl on convulsant activity seem to be dependent on the experimental animal model as well as the dose regimen.

[^{18}F]FDG PET is one of the most commonly used neuroimaging techniques in epileptic patients that allows for the evaluation of early glucose metabolic changes in relationship to synaptic and neuronal activity (Rocher et al., 2003). Interictal [^{18}F]-FDG PET features glucose hypometabolism in the epileptogenic region. Furthermore, the severity of seizures seems to relate to the degree of hypometabolism and it has been suggested that reciprocal positive feedback exists between seizures and hypometabolism (Blázquez et al., 2022; Gaillard et al., 2002; Zilberter and Zilberter, 2017). Importantly, interictal brain glucose hypometabolism has been consistently reproduced in the silent latent period of the lithium-pilocarpine model of SE (Bascuñana et al., 2021; García-García et al., 2017, 2016; Shiha et al., 2015). Although the exact mechanisms underpinning interictal glucose hypometabolism still remain unclear, neuronal loss, reduced synaptic density and altered cerebral blood flow have been involved. Our current data corroborates that the SE induced by pilocarpine results in glucose hypometabolism in epilepsy-related brain areas (Fig. 4). Furthermore, acute naftidrofuryl administration effectively ameliorates brain glucose hypometabolism

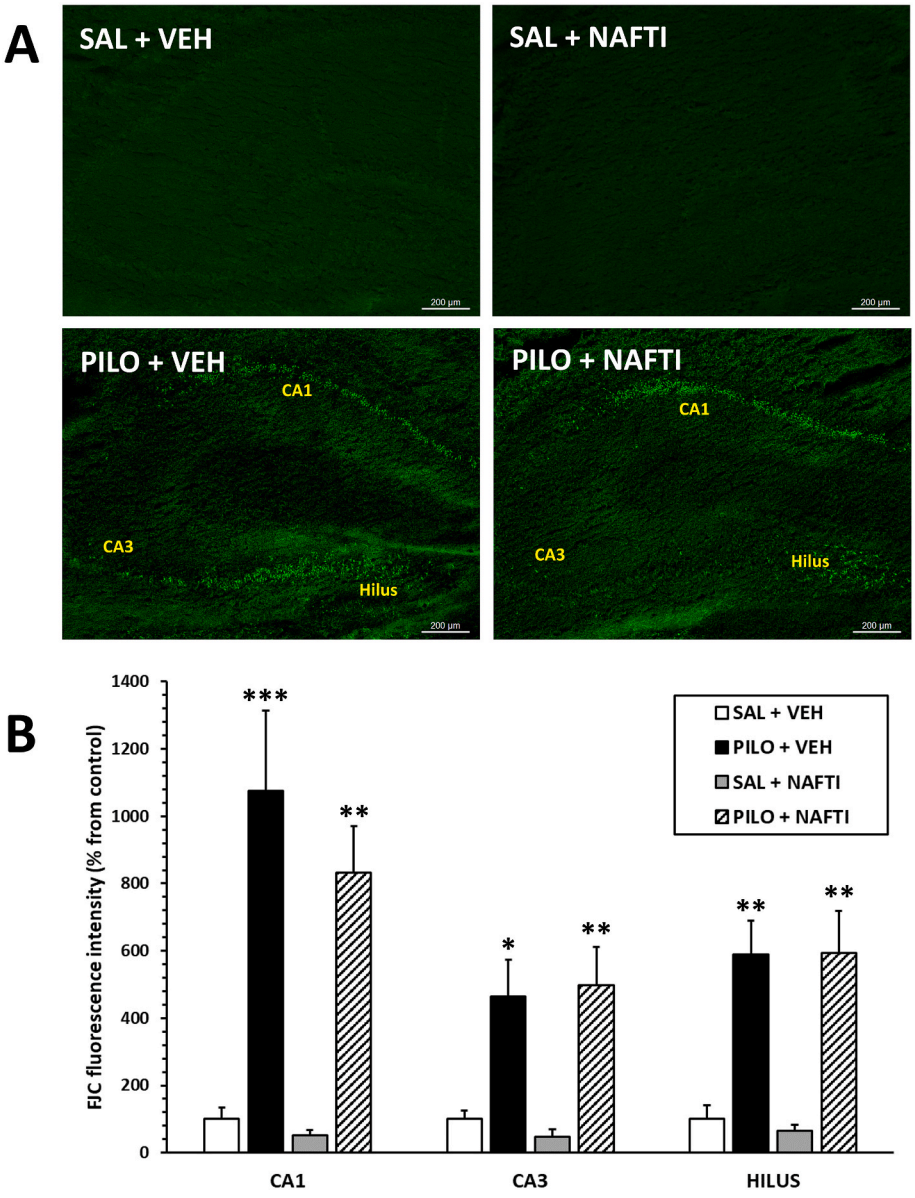

Fig. 6. Pilocarpine induced marked hippocampal neurodegeneration, which was not reduced by naftidrofuryl administration, as detected by Fluoro Jade C labeling. **(A)** Representative images of the hippocampus from the 4 experimental groups, 3 days after the SE. **(B)** Bar plot corresponding to Fluoro-Jade C fluorescence intensity values as marker of neurodegeneration. Data are expressed as percentage of the signal obtained in the SAL + VEH group and shown as mean ± SEM. *p<0.05, **p<0.01 and ***p<0.001 when compared to their respective control (vehicle treated groups); two-way ANOVAs followed by post-hoc Tukey test.

induced by SE (Fig. 4). Regarding cerebral blood flow in epilepsy, single photon emission computed tomography (SPECT) studies in humans using the radiophamaceutical tracer compound ^{99}mTc-Hexamethylpropyleneamine Oxime (^{99}mTc-HMPAO) have shown either interictal hypoperfusion or normal perfusion in the epileptogenic region (Kumar and Chugani, 2017a, 2017b). Similarly, in the rat lithium-pilocarpine model of SE, a recent ^{99}mTc-HMPAO SPECT neuroimaging study has reported that brain regional hypoperfusion emerges 15 min after the pilocarpine administration (i.e. before reaching SE) and becomes chronic, been detectable up to, at least, 12 weeks later (Bascuñana et al., 2021). In the clinical context, impaired cerebral blood flow and glucose hypometabolism concur in many neurological disorders. It has been proposed that the use of vasodilators such as naftidrofuryl might improve cerebral blood flow and therefore contribute to ameliorate the cognitive decline in these neurological diseases (Daulatzai, 2017; Emeriau et al., 2000). Herein, it is also important to bear in mind both, that epilepsy patients frequently suffer from cognitive impairment, psychiatric and mood disorders (Jensen, 2011) and that epileptic seizures also occur in many other neurological conditions, with a wide variety of etiologies and risk factors, being commonly concurrent with ischemic stroke and traumatic brain injury (Temkin, 2009).

Neuroinflammation, an adaptive physiological response to brain cell damage or loss and, gliosis affecting both astrocytes and microglia have been reported in epileptic disorders. It has been also suggested that brain glucose hypometabolism and neuroinflammation may act in concert, contributing to the establishment of the pathology. Neuroinflammation is also a feature of the lithium-pilocarpine rodent model (Bulduk et al., 2019; García-García et al., 2017) as well as of other animal models of acute seizures (García-García et al., 2018; Jupp et al., 2012). In agreement with previously reported studies obtained by our group (García-García et al., 2017, 2016; Shiha et al., 2015), our present data show that SE resulted in hippocampal neuronal damage as revealed by Nissl histological observations (Fig. 5) and increased Fluoro-Jade C signal (Fig. 6). Besides, SE triggered reactive astrogliosis, characterized by increased TRITC-GFAP fluorescence, hypertrophy, and proliferation (Fig. 7) and resulted in microglia-mediated neuroinflammation. [^{3}H]PK11195 autoradiographic studies provide measurements of microglial activation associated with mitochondrial overexpression of the peripheral-type benzodiazepine receptor, currently known as 18 kDa translocator protein (TSPO) (Papadopoulos et al., 2006). We show that SE resulted in increased [^{3}H]PK11195 binding (Fig. 8) which agrees with previous studies reporting increased [^{18}F]GE180 (a TSPO PET

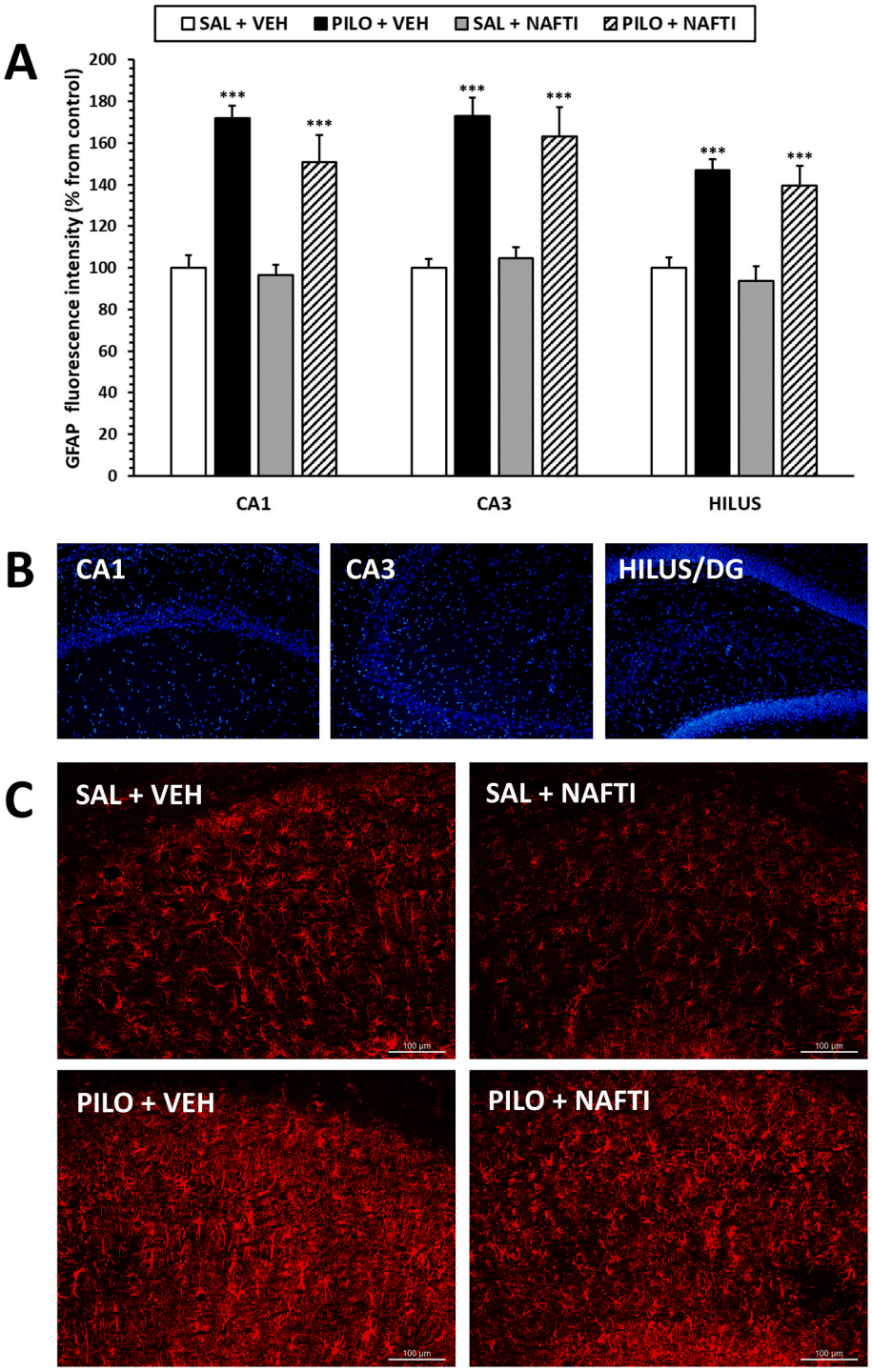

Fig. 7. Naftidrofuryl did not reduce astroglial reactivity in response to the SE triggered by pilocarpine. **(A)** Graph showing the astrocyte activation as TRITC fluorescence intensity (% from SAL + VEH group); ***$p<0.001$ *vs.* their respective control groups. **(B)** Representative DAPI-labelled images corresponding to CA1, CA3 and hilus/dentate gyrus used for precise localization and quantification of GFAP immunofluorescence in these hippocampal subregions. **(C)** Representative GFAP immunofluorescence micrographs at the level of CA1 of the 4 experimental groups, showing the intense astrocyte reactivity triggered by pilocarpine. As shown, naftidrofuryl administration (2 × 25 mg/kg) resulted in no reduction of such glial activation.

tracer) signal when neuronal damage occurs as consequence of seizures and epileptogenesis (Brackhan et al., 2018; García-García et al., 2018, 2017). Besides, the brain slices obtained from pilocarpine-insulted rats showed wide edematous areas, especially at the level of piriform and entorhinal cortices area as previously described (Kim et al., 2010). This edema formation was also evident at the hippocampus of many SE-damaged rats. Although, it has been suggested that counteracting the cerebral hypoperfusion during SE in the lithium-pilocarpine model may result in a reduced neurodegeneration and neuroinflammation (Bascuñana et al., 2021), our study on the effects of acute naftidrofuryl administration does not support either neuroprotective or antiinflammatory effects. Considering that in this model, seizure-induced brain damage is caused by glutamate-mediated excitotoxicity (Cavalheiro et al., 1994; Costa et al., 2004), reduced brain perfusion and increased brain energy requirements (Farrell et al., 2017), the acute improvement in brain blood perfusion by itself seems to be unable to lessen the SE-induced brain damage. Consequently, other complementary treatments might be necessary to comprehensively tackle the multi-factorial processes underpinning brain damage.

5. Conclusions

To sum up, as far as we know, this is the first time that functional neuroimaging PET has been applied to assess the effect of naftidrofuryl

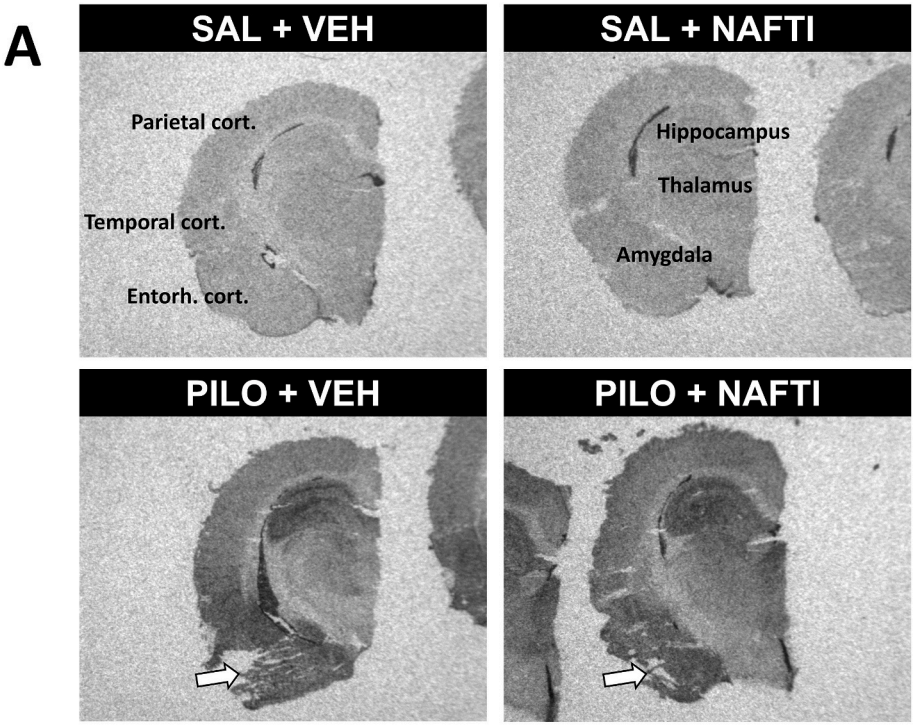

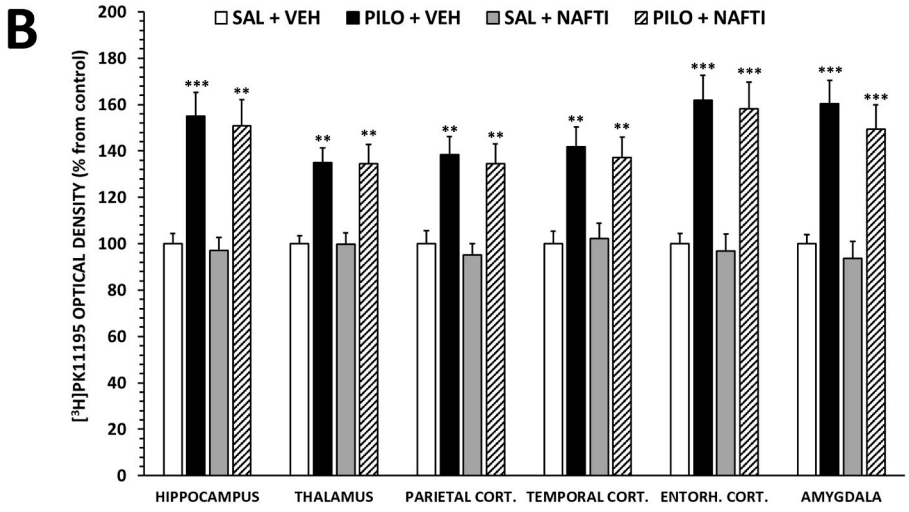

Fig. 8. Neuroinflammation induced by in SE, measured by the [^{3}H]PK11195 binding, in major brain regions involved in epileptogenesis was not reduced by acute administration of naftidrofuryl. **(A)** Representative [^{3}H]PK11195 autoradiograms corresponding to the 4 experimental groups obtained from the anterior hippocampus. The white arrows point to the edematous area at the piriform and entorhinal cortices by pilocarpine-induced SE. **(B)** Quantification of the [^{3}H]PK11195-TSPO binding (expressed in % O.D. change from PILO + VEH group and shown as mean ± SEM). ***p<0.001 PILO + VEH *vs.* SAL + VEH and PILO + NAFTI *vs.* SAL + NAFTI; two-way ANOVAs followed by post-hoc Tukey test.

on brain glucose hypometabolism induced by SE in the lithium-pilocarpine rat model. Our study does not support acute i.p. naftidrofuryl having antiseizure properties, neither neuroprotective nor anti-inflammatory effects. Nonetheless, naftidrofuryl treatment did significantly reduce brain glucose hypometabolism during the silent period that follows SE. Therefore, further studies are needed to determine whether longer treatments providing chronic improved blood flow in the lithium-pilocarpine model of SE together with other therapeutic approaches aimed to neuroprotection might eventually lead to beneficial consequences on neurodegeneration and/or neuroinflammation. Likewise, studies on less severe models of epileptogenesis might be a complementary alternative to further dissect the potential beneficial effects of naftidrofuryl in this neurological disorder.

CRediT authorship contribution statement

Luis García-García: Conceptualization, Methodology, Investigation, Formal analysis, Data curation, Visualization, Writing – original draft, preparation, Writing – review & editing. **Francisca Gomez:** Supervision, Formal analysis, Data curation, Visualization, Writing – original draft, preparation, Writing – review & editing. **Mercedes Delgado:** Investigation, Data curation. **Rubén Fernández de la Rosa:** Investigation, Data curation, Visualization. **Miguel Ángel Pozo:** Resources, Funding acquisition, Project administration.

Declaration of competing interest

none.

Data availability

Data will be made available on request.

Acknowledgements

This work was financially supported by the Spanish Ministerio de Ciencia e Innovación (Retos PID2019-106968RB-100).

References

Admani, A.K., 1978. New approach to treatment of recent stroke. Br. Med. J. 2, 1678–1679. https://doi.org/10.1136/BMJ.2.6153.1678.

Bascuñana, P., Wolf, B.J., Jahreis, I., Brackhan, M., García-García, L., Ross, T.L., Bengel, F.M., Bankstahl, M., Bankstahl, J.P., 2021. 99m Tc-HMPAO SPECT imaging reveals brain hypoperfusion during status epilepticus. Metab. Brain Dis. 36, 2597–2602. https://doi.org/10.1007/S11011-021-00843-Z.

Becker, A.J., 2018. Review: animal models of acquired epilepsy: insights into mechanisms of human epileptogenesis. Neuropathol. Appl. Neurobiol. 44, 112–129. https://doi.org/10.1111/NAN.12451.

Berg, A.T., Berkovic, S.F., Brodie, M.J., Buchhalter, J., Cross, J.H., van Emde Boas, W., Engel, J., French, J., Glauser, T.A., Mathern, G.W., Moshé, S.L., Nordli, D., Plouin, P., Scheffer, I.E., 2010. Revised terminology and concepts for organization of seizures and epilepsies: report of the ILAE Commission on Classification and Terminology, 2005-2009. Epilepsia 51, 676–685. https://doi.org/10.1111/J.1528-1167.2010.02522.X.

Blázquez, E., Hurtado-Carneiro, V., LeBaut-Ayuso, Y., Velázquez, E., García-García, L., Gómez-Oliver, F., Ruiz-Albusac, J.M., Ávila, J., Pozo, M.Á., 2022. Significance of brain glucose hypometabolism, altered insulin signal transduction, and insulin resistance in several neurological diseases. Front. Endocrinol. 13 https://doi.org/10.3389/FENDO.2022.873301.

Brackhan, M., Bascuñana, P., Ross, T.L., Bengel, F.M., Bankstahl, J.P., Bankstahl, M., 2018. [18 F]GE180 positron emission tomographic imaging indicates a potential double-hit insult in the intrahippocampal kainate mouse model of temporal lobe epilepsy. Epilepsia 59, 617–626. https://doi.org/10.1111/EPI.14009.

Buckmaster, P.S., 2004. Laboratory animal models of temporal lobe epilepsy. Comp. Med. 54, 473–485.

Bulduk, E.B., Kurt, G., Barun, S., Aydemir, O., Kiziltas, M., Oktem, M., Turhan, T., Atilla, P., Muftuoglu, S., 2019. The effects of minocycline on the Hippocampus in lithium- pilocarpine induced status epilepticus in rat: relations with microglial/astrocytic activation and serum S100B level. Turk Neurosurg 29, 95–105. https://doi.org/10.5137/1019-5149.JTN.22744-18.1.

Cavalheiro, E.A., Fernandes, M.J., Turski, L., Naffah-Mazzacoratti, M.G., 1994. Spontaneous recurrent seizures in rats: amino acid and monoamine determination in the hippocampus. Epilepsia 35, 1–11. https://doi.org/10.1111/J.1528-1157.1994.TB02905.X.

Costa, M.S., Rocha, J.B.T., Perosa, S.R., Cavalheiro, E.A., Naffah-Mazzacoratti, M.D.G., 2004. Pilocarpine-induced status epilepticus increases glutamate release in rat hippocampal synaptosomes. Neurosci. Lett. 356, 41–44. https://doi.org/10.1016/j.neulet.2003.11.019.

Cox, J.R., 1975. Double-blind evaluation of naftidrofuryl in treating elderly confused hospitalised patients. Gerontol. Clin. 17, 160–167. https://doi.org/10.1159/000245573.

Curia, G., Longo, D., Biagini, G., Jones, R.S.G., Avoli, M., 2008. The pilocarpine model of temporal lobe epilepsy. J. Neurosci. Methods 172, 143–157. https://doi.org/10.1016/j.jneumeth.2008.04.019.

Daulatzai, M.A., 2017. Cerebral hypoperfusion and glucose hypometabolism: key pathophysiological modulators promote neurodegeneration, cognitive impairment, and Alzheimer's disease. J. Neurosci. Res. 95, 943–972. https://doi.org/10.1002/JNR.23777.

Emeriau, J.P., Lehert, P., Mosnier, M., 2000. Efficacy of naftidrofuryl in patients with vascular or mixed dementia: results of a multicenter, double-blind trial. Clin. Therapeut. 22, 834–844. https://doi.org/10.1016/S0149-2918(00)80056-9.

Endemann, D., Schweda, F., Stubanus, M., Ittner, K.P., Fischereder, M., Kammerl, M.C., Krämer, B.K., 2002. Naftidrofuryl exerts antiserotonergic but no endothelin-receptor blocking effects in AS4.1 cells, juxtaglomerular cells and isolated perfused rat kidneys. J. Cardiovasc. Pharmacol. 39, 1–8. https://doi.org/10.1097/00005344-200201000-00001.

Farrell, J.S., Colangeli, R., Wolff, M.D., Wall, A.K., Phillips, T.J., George, A., Federico, P., Teskey, G.C., 2017. Postictal hypoperfusion/hypoxia provides the foundation for a unified theory of seizure-induced brain abnormalities and behavioral dysfunction. Epilepsia 58, 1493–1501. https://doi.org/10.1111/EPI.13827.

Fisher, R.S., Acevedo, C., Arzimanoglou, A., Bogacz, A., Cross, J.H., Elger, C.E., Engel, J., Forsgren, L., French, J.A., Glynn, M., Hesdorffer, D.C., Lee, B.I., Mathern, G.W., Moshé, S.L., Perucca, E., Scheffer, I.E., Tomson, T., Watanabe, M., Wiebe, S., 2014. ILAE official report: a practical clinical definition of epilepsy. Epilepsia 55, 475–482. https://doi.org/10.1111/EPI.12550.

Foucault-Fruchard, L., Doméné, A., Page, G., Windsor, M., Emond, P., Rodrigues, N., Dollé, F., Damont, A., Buron, F., Routier, S., Chalon, S., Antier, D., 2017. Neuroprotective effect of the alpha 7 nicotinic receptor agonist PHA 543613 in an in vivo excitotoxic adult rat model. Neuroscience 356, 52–63. https://doi.org/10.1016/J.NEUROSCIENCE.2017.05.019.

Gaillard, W.D., Kopylev, L., Weinstein, S., Conry, J., Pearl, P.L., Spanaki, M.v., Fazilat, S., Fazilat, S., Venzina, L.G., Dubovsky, E., Theodore, W.H., 2002. Low incidence of abnormal (18)FDG-PET in children with new-onset partial epilepsy: a prospective study. Neurology 58, 717–722. https://doi.org/10.1212/WNL.58.5.717.

García-García, L., Fernández de la Rosa, R., Delgado, M., Silván, Á., Bascuñana, P., Bankstahl, J.P., Gomez, F., Pozo, M.A., 2018. Metyrapone prevents acute glucose hypermetabolism and short-term brain damage induced by intrahippocampal administration of 4-aminopyridine in rats. Neurochem. Int. 113, 92–106. https://doi.org/10.1016/J.NEUINT.2017.11.018.

García-García, L., Shiha, A.A., Bascuñana, P., de Cristóbal, J., Fernández de la Rosa, R., Delgado, M., Pozo, M.A., 2016. Serotonin depletion does not modify the short-term brain hypometabolism and hippocampal neurodegeneration induced by the lithium-pilocarpine model of status epilepticus in rats. Cell. Mol. Neurobiol. 36, 513–519. https://doi.org/10.1007/S10571-015-0240-4.

García-García, L., Shiha, A.A., Fernández de la Rosa, R., Delgado, M., Silván, Á., Bascuñana, P., Bankstahl, J.P., Gomez, F., Pozo, M.A., 2017. Metyrapone prevents brain damage induced by status epilepticus in the rat lithium-pilocarpine model. Neuropharmacology 123, 261–273. https://doi.org/10.1016/J.NEUROPHARM.2017.05.007.

Gerin, J., 1974. Double-blind trial of naftidrofuryl in the treatment of cerebral arteriosclerosis. Br. J. Clin. Pract. 28, 177–178.

Jagroop, I.A., Mikhailidis, D.P., 2000. Effect of endothelin-1 on human platelet shape change: reversal of activation by naftidrofuryl. Platelets 11, 272–277. https://doi.org/10.1080/09537100050129288.

Janszky, J., Janszky, I., Schulz, R., Hoppe, M., Behne, F., Pannek, H.W., Ebner, A., 2005. Temporal lobe epilepsy with hippocampal sclerosis: predictors for long-term surgical outcome. Brain 128, 395–404. https://doi.org/10.1093/BRAIN/AWH358.

Jensen, F.E., 2011. Epilepsy as a spectrum disorder: implications from novel clinical and basic neuroscience. Epilepsia 52 (Suppl. 1), 1–6. https://doi.org/10.1111/J.1528-1167.2010.02904.X.

Judge, T.G., Urquhart, A.G., 1972. Naftidrofuryl–a double blind cross-over study in the elderly. Curr. Med. Res. Opin. 1, 166–172. https://doi.org/10.1185/03007997209111162.

Jupp, B., Williams, J., Binns, D., Hicks, R.J., Cardamone, L., Jones, N., Rees, S., O'Brien, T.J., 2012. Hypometabolism precedes limbic atrophy and spontaneous recurrent seizures in a rat model of TLE. Epilepsia 53, 1233–1244. https://doi.org/10.1111/J.1528-1167.2012.03525.X.

Kandratavicius, L., Alves Balista, P., Lopes-Aguiar, C., Ruggiero, R.N., Umeoka, E.H., Garcia-Cairasco, N., Bueno-Junior, L.S., Leite, J.P., 2014. Animal models of epilepsy: use and limitations. Neuropsychiatric Dis. Treat. 10, 1693–1705. https://doi.org/10.2147/NDT.S50371.

Kim, J.E., Yeo, S. ll, Ryu, H.J., Kim, M.J., Kim, D.S., Jo, S.M., Kang, T.C., 2010. Astroglial loss and edema formation in the rat piriform cortex and hippocampus following pilocarpine-induced status epilepticus. J. Comp. Neurol. 518, 4612–4628. https://doi.org/10.1002/CNE.22482.

Kumar, A., Chugani, H.T., 2017a. The role of radionuclide imaging in epilepsy, part 2: epilepsy syndromes. J. Nucl. Med. Technol. 45, 294–301. https://doi.org/10.2967/jnumed.113.129593.

Kumar, A., Chugani, H.T., 2017b. The role of radionuclide imaging in epilepsy, part 1: sporadic temporal and extratemporal lobe epilepsy. J. Nucl. Med. Technol. 45, 286–293. https://doi.org/10.2967/jnumed.112.114397.

Lee, E.M., Park, G.Y., Im, K.C., Kim, S.T., Woo, C.W., Chung, J.H., Kim, K.S., Kim, J.S., Shon, Y.M., Kim, Y.I., Kang, J.K., 2012. Changes in glucose metabolism and metabolites during the epileptogenic process in the lithium-pilocarpine model of epilepsy. Epilepsia 53, 860–869. https://doi.org/10.1111/J.1528-1167.2012.03432.X.

Leite, J.P., Garcia-Cairasco, N., Cavalheiro, E.A., 2002. New insights from the use of pilocarpine and kainate models. Epilepsy Res. 50, 93–103. https://doi.org/10.1016/S0920-1211(02)00072-4.

Lu, D., Song, H., Hao, Z., Wu, T., McCleery, J., 2011. Naftidrofuryl for dementia. Cochrane Database Syst. Rev. https://doi.org/10.1002/14651858.CD002955.PUB4.

Maloteaux, J.M., Haiech, J., de Campeneere, D., Berta, P., Vidal, N., 1986. Biochemical and physiological evidences for antiserotonergic properties of naftidrofuryl. Arzneimittelforschung 36, 1194–1198.

Miyake, K., Tanonaka, K., Nasa, Y., Takagi, N., Tsuchiya, T., Yoshizawa, M., Fujioka, Y., Takeo, S., 1993. Effects of naftidrofuryl oxalate on microsphere embolism-induced changes in tricarboxylic acid cycle intermediates of rats. Eur. J. Pharmacol. 235, 75–81. https://doi.org/10.1016/0014-2999(93)90822-Y.

Ogawa, S. ichi, Kameyama, T., Nabeshima, T., 1991. Naftidrofuryl oxalate, nootropic effects on the scopolamine- and the basal forebrain lesion-induced amnesia in rats. Pharmacol. Biochem. Behav. 39, 997–1002. https://doi.org/10.1016/0091-3057(91)90065-A.

Oudart, N., 1990. Naftidrofuryl inhibits contractions to serotonin in intact and de-endothelialized cerebral arteries in vitro. J. Cardiovasc. Pharmacol. 16, S45–S48. https://doi.org/10.1097/00005344-199000163-00011.

Papadopoulos, V., Baraldi, M., Guilarte, T.R., Knudsen, T.B., Lacapère, J.J., Lindemann, P., Norenberg, M.D., Nutt, D., Weizman, A., Zhang, M.R., Gavish, M., 2006. Translocator protein (18kDa): new nomenclature for the peripheral-type benzodiazepine receptor based on its structure and molecular function. Trends Pharmacol. Sci. 27, 402–409. https://doi.org/10.1016/J.TIPS.2006.06.005.

Pohlmann-Eden, B., Linden, D., Bergler, W., 1991. [Convulsive crises and cardiovascular complications following high-dosage parenteral administration of naftidrofuryl]. Dtsch. Med. Wochenschr. 116, 1453.

Racine, R.J., 1972. Modification of seizure activity by electrical stimulation. II. Motor seizure. Electroencephalogr. Clin. Neurophysiol. 32, 281–294. https://doi.org/10.1016/0013-4694(72)90177-0.

Rigoulot, M.A., Koning, E., Ferrandon, A., Nehlig, A., 2004. Neuroprotective properties of topiramate in the lithium-pilocarpine model of epilepsy. J. Pharmacol. Exp. Therapeut. 308, 787–795. https://doi.org/10.1124/JPET.103.057091.

Rocher, A.B., Chapon, F., Blaizot, X., Baron, J.C., Chavoix, C., 2003. Resting-state brain glucose utilization as measured by PET is directly related to regional synaptophysin

levels: a study in baboons. Neuroimage 20, 1894. https://doi.org/10.1016/J.NEUROIMAGE.2003.07.002. –1898.
Rossi, A.R., Angelo, M.F., Villarreal, A., Lukin, J., Ramos, A.J., 2013. Gabapentin administration reduces reactive gliosis and neurodegeneration after pilocarpine-induced status epilepticus. PLoS One 8. https://doi.org/10.1371/JOURNAL.PONE.0078516.
Samokhina, E., Samokhin, A., 2018. Neuropathological profile of the pentylenetetrazol (PTZ) kindling model. Int. J. Neurosci. 128, 1086–1096. https://doi.org/10.1080/00207454.2018.1481064.
Sarikaya, I., 2015. PET studies in epilepsy. Am J Nucl Med Mol Imaging 5, 416–430.
Schmidt, J., 1990. Comparative studies on the anticonvulsant effectiveness of nootropic drugs in kindled rats. Biomed. Biochim. Acta 49, 413–419.
Schmued, L.C., Stowers, C.C., Scallet, A.C., Xu, L., 2005. Fluoro-Jade C results in ultra high resolution and contrast labeling of degenerating neurons. Brain Res. 1035, 24–31. https://doi.org/10.1016/J.BRAINRES.2004.11.054.
Shapiro, L.A., Wang, L., Ribak, C.E., 2008. Rapid astrocyte and microglial activation following pilocarpine-induced seizures in rats. Epilepsia 49 (Suppl. 2), 33–41. https://doi.org/10.1111/J.1528-1167.2008.01491.X.
Shiha, A.A., de Cristóbal, J., Delgado, M., Fernández de la Rosa, R., Bascuñana, P., Pozo, M.A., García-García, L., 2015. Subacute administration of fluoxetine prevents short-term brain hypometabolism and reduces brain damage markers induced by the lithium-pilocarpine model of epilepsy in rats. Brain Res. Bull. 111, 36–47. https://doi.org/10.1016/J.BRAINRESBULL.2014.12.009.
Shultz, S.R., Cardamone, L., Liu, Y.R., Edward Hogan, R., MacCotta, L., Wright, D.K., Zheng, P., Koe, A., Gregoire, M.C., Williams, J.P., Hicks, R.J., Jones, N.C., Myers, D. E., O'Brien, T.J., Bouilleret, V., 2013. Can structural or functional changes following traumatic brain injury in the rat predict epileptic outcome? Epilepsia 54, 1240–1250. https://doi.org/10.1111/EPI.12223.
Slowing, K., Gomez, F., Delgado, M., Fernández de la Rosa, R., Hernández-Martín, N., Pozo, M.A., García-García, L., 2022. PET imaging and neurohistochemistry reveal that curcumin attenuates brain hypometabolism and hippocampal damage induced by status epilepticus in rats. Planta Med. https://doi.org/10.1055/a-1948-4378.
Taguchi, T., Takagi, N., Miyake, K., Tanonaka, K., Okada, M., Kajihara, H., Takeo, S., 1994. Effects of naftidrofuryl oxalate on microsphere-induced changes in acetylcholine and amino acid content of rat brain regions. Exp. Brain Res. 99, 7–16. https://doi.org/10.1007/BF00241407.
Tang, F., Hartz, A.M.S., Bauer, B., 2017. Drug-resistant epilepsy: multiple hypotheses, few answers. Front. Neurol. 8 https://doi.org/10.3389/FNEUR.2017.00301.
Téllez-Zenteno, J.F., Hernández-Ronquillo, L., 2012. A review of the epidemiology of temporal lobe epilepsy, 2012 Epilepsy Res Treat 1–5. https://doi.org/10.1155/2012/630853.
Temkin, N.R., 2009. Preventing and treating posttraumatic seizures: the human experience. Epilepsia 50 (Suppl. 2), 10–13. https://doi.org/10.1111/J.1528-1167.2008.02005.X.
Turski, W.A., Cavalheiro, E.A., Schwarz, M., Czuczwar, S.J., Kleinrok, Z., Turski, L., 1983. Limbic seizures produced by pilocarpine in rats: behavioural, electroencephalographic and neuropathological study. Behav. Brain Res. 9, 315–335. https://doi.org/10.1016/0166-4328(83)90136-5.
Walton, N.Y., Treiman, D.M., 1988. Response of status epilepticus induced by lithium and pilocarpine to treatment with diazepam. Exp. Neurol. 101, 267–275. https://doi.org/10.1016/0014-4886(88)90010-6.
Wiernsperger, N.F., 1994. Serotonin, 5-HT2receptors, and their blockade by naftidrofuryl: a targeted therapy of vascular diseases. J. Cardiovasc. Pharmacol. 23, S37–S43. https://doi.org/10.1097/00005344-199406030-00008.
Yang, Y., Guo, Y., Kuang, Y., Wang, Shan, Jiang, Y., Ding, Y., Wang, Shuang, Ding, M., 2014. Serotonin 1A receptor inhibits the status epilepticus induced by lithium-pilocarpine in rats. Neurosci. Bull. 30, 401–408. https://doi.org/10.1007/s12264-013-1396-x.
Young, A.R., Barry, D.I., MacKenzie, E.T., Robert, J.P., 1983. Cerebro-circulatory effects of so-called "vasodilators" in the anaesthetised rat. Eur. Neurol. 22, 142–153. https://doi.org/10.1159/000115551.
Zhang, L., Guo, Y., Hu, H., Wang, J., Liu, Z., Gao, F., 2015. FDG-PET and NeuN-GFAP immunohistochemistry of hippocampus at different phases of the pilocarpine model of temporal lobe epilepsy. Int. J. Med. Sci. 12, 288–294. https://doi.org/10.7150/IJMS.10527.
Zilberter, Y., Zilberter, M., 2017. The vicious circle of hypometabolism in neurodegenerative diseases: ways and mechanisms of metabolic correction. J. Neurosci. Res. 95, 2217–2235. https://doi.org/10.1002/JNR.24064.